Hindawi
Structural Control and Health Monitoring
Volume 2023, Article ID 4950487, 13 pages
https://doi.org/10.1155/2023/4950487

*Research Article*

# A Multistep Direct and Indirect Strategy for Predicting Wind Direction Based on the EMD-LSTM Model

**Yang Ding**,[1,2,3] **Xiao-Wei Ye**,[4] **and Yong Guo**[5]

[1]*Zhejiang Engineering Research Center of Intelligent Urban Infrastructure, Hangzhou City University, Hangzhou 310015, China*
[2]*Key Laboratory of Safe Construction and Intelligent Maintenance for Urban Shield Tunnels of Zhejiang Province, Hangzhou City University, Hangzhou 310015, China*
[3]*Department of Civil Engineering, Hangzhou City University, Hangzhou 310015, China*
[4]*Department of Civil Engineering, Zhejiang University, Hangzhou 310058, China*
[5]*Zhejiang Jiashao Bridge Investment and Development Co., Ltd., Shaoxing 312366, China*

Correspondence should be addressed to Yang Ding; ceyangding@zju.edu.cn

Received 22 September 2022; Revised 10 March 2023; Accepted 5 April 2023; Published 28 April 2023

Academic Editor: Suparno Mukhopadhyay



For the wind speed prediction, many researchers have established prediction models based on machine learning methods, statistical methods, and theoretical methods, that is, direct methods. However, the direct method cannot be widely used in the wind direction prediction because the wind direction has strong randomness and uncertainty. In order to solve this problem, this paper proposed a wind direction prediction method, that is, indirect method. Specifically, the wind speed is decomposed into crosswind speed and alongwind speed considering the correlation between wind speed and wind direction. The crosswind speed and alongwind speed are predicted based on long short-term memory (LSTM) model with empirical mode decomposition (EMD), and then, the wind direction prediction value can be calculated, that is, the wind direction prediction is realized. One-month wind monitoring data collected by the structural health monitoring (SHM) system installed on investigated bridge are employed to demonstrate the effectiveness of direct and indirect prediction for forecasting the wind speed and wind direction.

## 1. Introduction

With the continuous advancements of modern bridges toward super long spans and extreme flexibility, the influence of wind on bridges is becoming more obvious, and it even plays a control role [1]. How to accurately predict wind load for long-span bridges during operation is critical for traffic control because excessive wind load will cause bridge vibration and may lead to traffic accidents [2].

To predict wind load, we need to first obtain a large amount of wind field data, i.e., wind speed and direction data [3]. Nowadays, the structural health monitoring (SHM) systems are installed on new long-span bridges to obtain wind field data [4]. For example (see Appendix B for detailed abbreviations), Xu et al. [5] estimated site-specific extreme wind speeds, structural temperatures, and traffic load effects of a long-span cable-stayed bridge using long-term SHM data and compared them with respective design values. Ye et al. [6] calculated full-scale wind field characteristics using field monitoring data from the SHM system of Xihoumen Bridge. Zhou and Sun [7] focused on the effects of high winds on vibrational responses and variation in modal parameters for a unique sea-crossing cable-stayed bridge, i.e., Donghai Bridge, using long-term SHM data.

In addition, an SHM system may be unstable, such as voltage instability, which will lead to noise in the obtained data (Li et al. [8]). Therefore, the SHM data should be preprocessed, that is, the data should be denoised [9]. At present, several methods can be used to denoise data. For example, Hu et al. [10] decomposed the original wind speed data into several independent intrinsic mode functions (IMFs) and one residual series by ensemble empirical mode decomposition (EEMD) using the principle of decomposition. Wu et al. [11] used complete EEMD to an

original wind speed sequence into a set of IMFs. Hu et al. [12] proposed a new data-driven model that combined variational mode decomposition and prediction models for daily streamflow forecasting. Pandey et al. [13] proposed an EEMD-difference pattern sequence forecasting method, which significantly outperformed other state-of-the-art methods in terms of prediction accuracy. Qian et al. [14] and Bokde et al. [15] reviewed the evolution of empirical mode decomposition (EMD)-based methods and novel techniques for treating IMFs generated by EMD/EEMD.

When wind speed and direction data are available, a prediction model needs to be established to predict them. In this regard, many researchers have predicted wind speed using machine learning methods, traditional theoretical analysis models, mathematical statistics, and these can be called direct methods. For example, Liu et al. [16] proposed a seasonal auto-regression integrated moving average (SARIMA) model to predict hourly measured wind speeds in the coastal/offshore area of Scotland. To verify the performance of the SARIMA model, it was compared with the newly developed deep learning-based algorithms of gated recurrent units and long- and short-term memory (LSTM). Shahid et al. [17] proposed a machine learning paradigm by exploiting the strength of recurrent neural networks based on LSTM, embedded with wavelet kernels, to encompass the dynamic behavior of temporal data. Liu et al. [18] proposed a novel hybrid short-term wind speed forecasting model based on singular spectrum analysis, convolutional neural networks, gated recurrent units, and support vector regression. Liu et al. [19] proposed three hybrid models, wavelet packets, time series analysis, and artificial neural networks (ANNs), to predict wind speed. Jung et al. [20] used ANNs to predict the long-term wind speeds of a particular site and to estimate the annual energy production of wind turbines using the predicted wind speeds. Guo et al. [21] developed a hybrid SARIMA and least square support vector machine model to predict the mean monthly wind speed in the Hexi Corridor.

These direct methods can accurately predict the wind speed. However, there are few reports on the wind direction prediction using direct methods, which could be due to the randomness and uncertainty of wind direction being greater than those of wind speed. Thus, direct methods cannot be applied to wind direction prediction (Ye et al. [22]; Alduse et al. [23]). In addition, the wind direction has a significant impact on the safe operation of bridges. On the one hand, the wind field environment at a bridge varies with wind direction, resulting in different vibration modes of the bridge, which may even lead to bridge damage. For example, Ding et al. [24] used finite element method software to investigate the influence of the wind direction on the wind field of bridge hangers. Wang et al. [25] conducted tests for a bridge deck under two wind directions during the completion and construction stages. The test and simulation results show that the properties of vortex-induced vibrations vary with the wind direction because of the asymmetry of the main girder. Xiang et al. [26] conducted a wind tunnel experiment to study wind loads acting on a moving vehicle model on a bridge installed with a solid wind barrier.

On the other hand, the calculation of wind load is not only related to the wind speed but also related to the wind direction; that is, the wind load under the combined action of wind speed and direction is greater than that under the action of wind speed. For example, Li et al. [27] presented a novel copula-based approach to model the joint cumulative distribution function of wind speed and direction for the wind-resistant design of engineering structures. Wang et al. [28] established a joint distribution of wind speed and direction for estimating the basic wind speed. It is shown that the calculated basic wind speed is reduced by considering the influence of the wind direction. The basic wind speed considering the influence of direction or not is significantly smaller than that in China's specification. Zhang and Chen [29] presented a new approach for estimating wind load effects (responses) for various mean recurrence intervals considering both the directionality and uncertainty of wind speed and wind load effects. Therefore, it is essential to predict the wind direction.

To overcome the challenges of wind direction prediction, this study establishes direct and indirect methods for predicting wind speed and direction, respectively, based on LSTM, which is seen as a benchmark model. First, we use the LSTM model to directly predict the wind speed and direction and observe its prediction performance, i.e., a direct method. Furthermore, the obtained wind data were denoised by EMD. Then, the wind speed is decomposed into crosswind and alongwind speeds considering the correlation between wind speed and direction. In addition, the crosswind and alongwind speeds are predicted by LSTM-EMD. Furthermore, the expression of wind direction is deduced based on the correlation between the wind speed and direction, and the wind direction is predicted, i.e., an indirect method.

## 2. Methodology

*2.1. Empirical Mode Decomposition.* The EMD method is obtained by interpolating a certain interval of data, i.e., selecting the maximum and minimum values of local data and calculating the average value of the local data (Qu et al. [30]). Then, we subtract the average value from the original data to obtain new data. As a result, the original data are gradually decomposed into the $(n-1)$ th IMF and residual value, which can be expressed as follows (Benbouzid [31]):

$$P(t) = \sum_{i=1}^{n-1} y_i(t) + l_n(t), \tag{1}$$

where $P(t)$ is the SHM data; $y_i(t)$ is the $i$th IMF; and $l_n(t)$ is the residual value (see Appendix A for detailed variables symbol).

*2.2. LSTM Prediction Model.* LSTM is a type of cyclic neural network that can analyze the input information based on the time series (Meng et al. [32]). In other words, it considers the correlation between the input information at the current and next times (Yuan et al. [33]). Generally, an LSTM network consists of an input gate, a forgetting gate, and an output

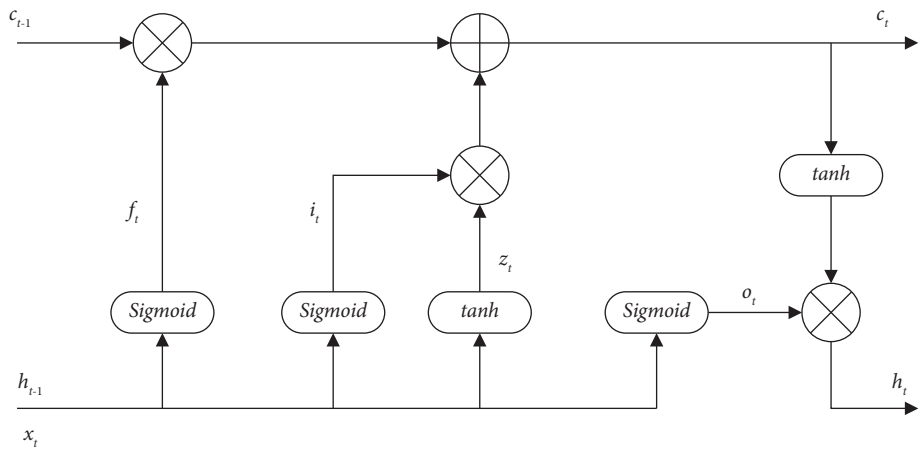


Figure 1: LSTM network.

Figure 2: Deployment of wind anemometers on the investigated bridge.

gate, as shown in Figure 1. The input gate saves the input information to the cell and creates a new state vector. The forgetting gate stores hidden state information about the previous unit in the current unit. The output gate outputs unit status information to the next unit (Xu et al. [34]).

Specifically, the parameters in Figure 1 can be expressed as follows (Zhang et al. [35]):

$$\begin{aligned} f_t &= \text{sigmoid}\left(W_f \times [h_{t-1}, x_t] + b_f\right), \\ i_t &= \text{sigmoid}\left(W_i \times [h_{t-1}, x_t] + b_i\right), \\ o_t &= \text{sigmoid}\left(W_o \times [h_{t-1}, x_t] + b_o\right), \\ z_t &= \tanh\left(W_z \times [h_{t-1}, x_t] + b_z\right), \\ c_t &= \left(c_{t-1} \times f_t\right) + \left(z_t \times i_t\right), \\ h_t &= \tanh\left(c_t\right) \times o_t, \end{aligned} \tag{2}$$

where $i_t$ denotes the input gate, and its weight and offset are denoted by $W_i$ and $b_i$, respectively; $f_t$ denotes the forgetting gate, and its weight and offset are denoted by $W_f$ and $b_f$, respectively; $o_t$ denotes the output gate, and its weight and offset are denoted by $W_o$ and $b_o$, respectively; $x_t$ denotes unit input; $z_t$ denotes the status of the temporary unit, and its weight and offset are denoted by $W_z$ and $b_z$ respectively; $c_t$ denotes the current unit state; $c_{t-1}$ denotes the status of the previous unit; $h_t$ denotes the hidden state of the current unit; $h_{t-1}$ denotes the hidden state of the previous unit.

*2.3. Prediction Performance Evaluation.* To evaluate the prediction performance of the model, the root mean square error (RMSE) is used to assess the performance of the wind speed and direction prediction model as follows (Ye et al. [36]):

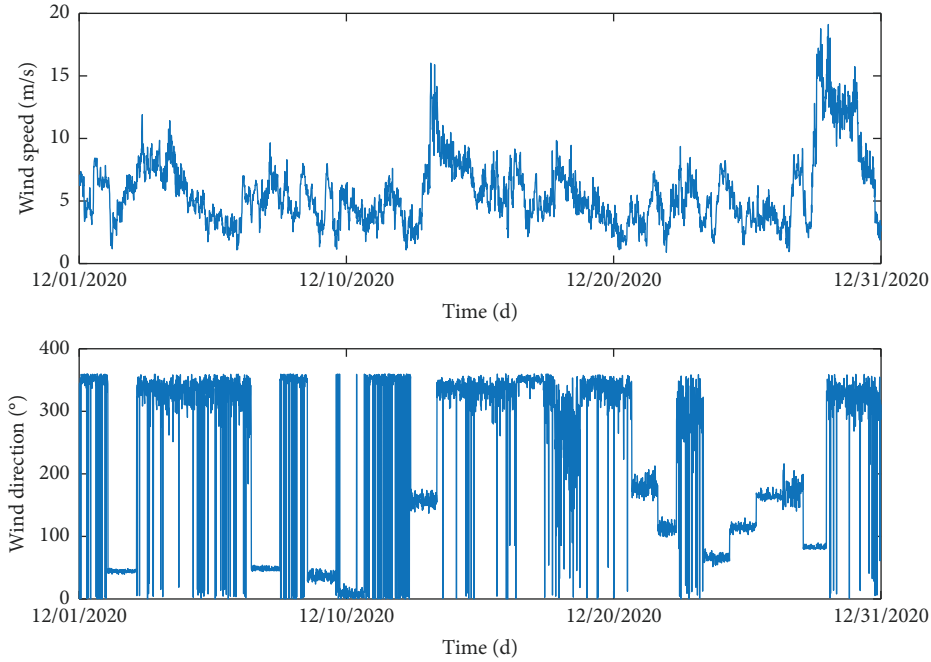


Figure 3: Wind monitoring data.

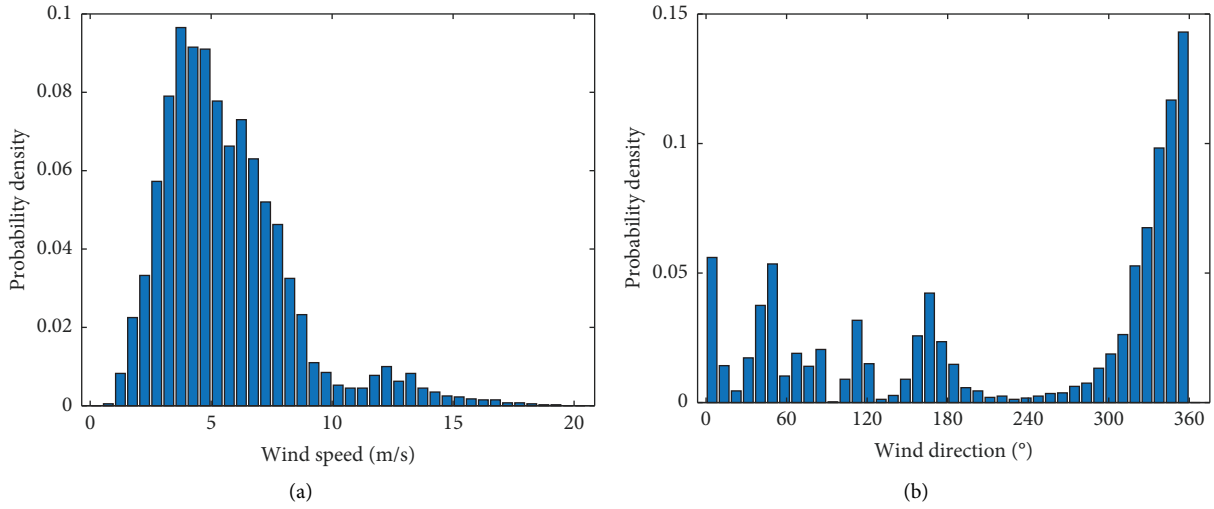


Figure 4: Statistical characteristics of wind data. (a) Statistical of wind speed. (b) Statistical of the wind direction.

$$\text{RMSE} = \sqrt{\frac{1}{N}\sum_{n=1}^{N}(y_n - Y_n)^2}, \tag{3}$$

where $y_n$ denotes the $n$th observation data point; $Y_n$ denotes the $n$th corresponding model prediction; and $N$ represents the size of the test set sample. Based on the definition of the RMSE rule, the smaller the RMSE value, the better the fit of the model.

## 3. Illustrative Application: Investigated Bridge

*3.1. Bridge and Its SHM Description.* An SHM system, i.e., an ultrasonic anemometer (UAN-G54-001-1), was installed to monitor the environmental wind around the bridge being investigated (Ding et al. [37]). In particular, the UAN is installed at a horizontal distance of 4 m from the bridge deck. The sampling frequency of the UAN is set as 10 Hz. The wind speeds of the UAN range from 0 to 60 m/s with a resolution of 0.01 m/s to ensure measurement accuracy. The UAN layout on the bridge being investigated is shown in Figure 2.

We use a UAN to collect wind speed and direction data of the Jiashao Bridge from December 1 to 31, 2020. During this period, the UAN collected 10 wind data points in 1 s. To facilitate data processing and analysis, we selected the maximum wind speed and its corresponding wind direction data every 10 min, i.e., extreme wind speed, as shown in Figure 3. Figure 3 shows that Jiashao Bridge experienced less strong wind during the study period, i.e., fewer times when

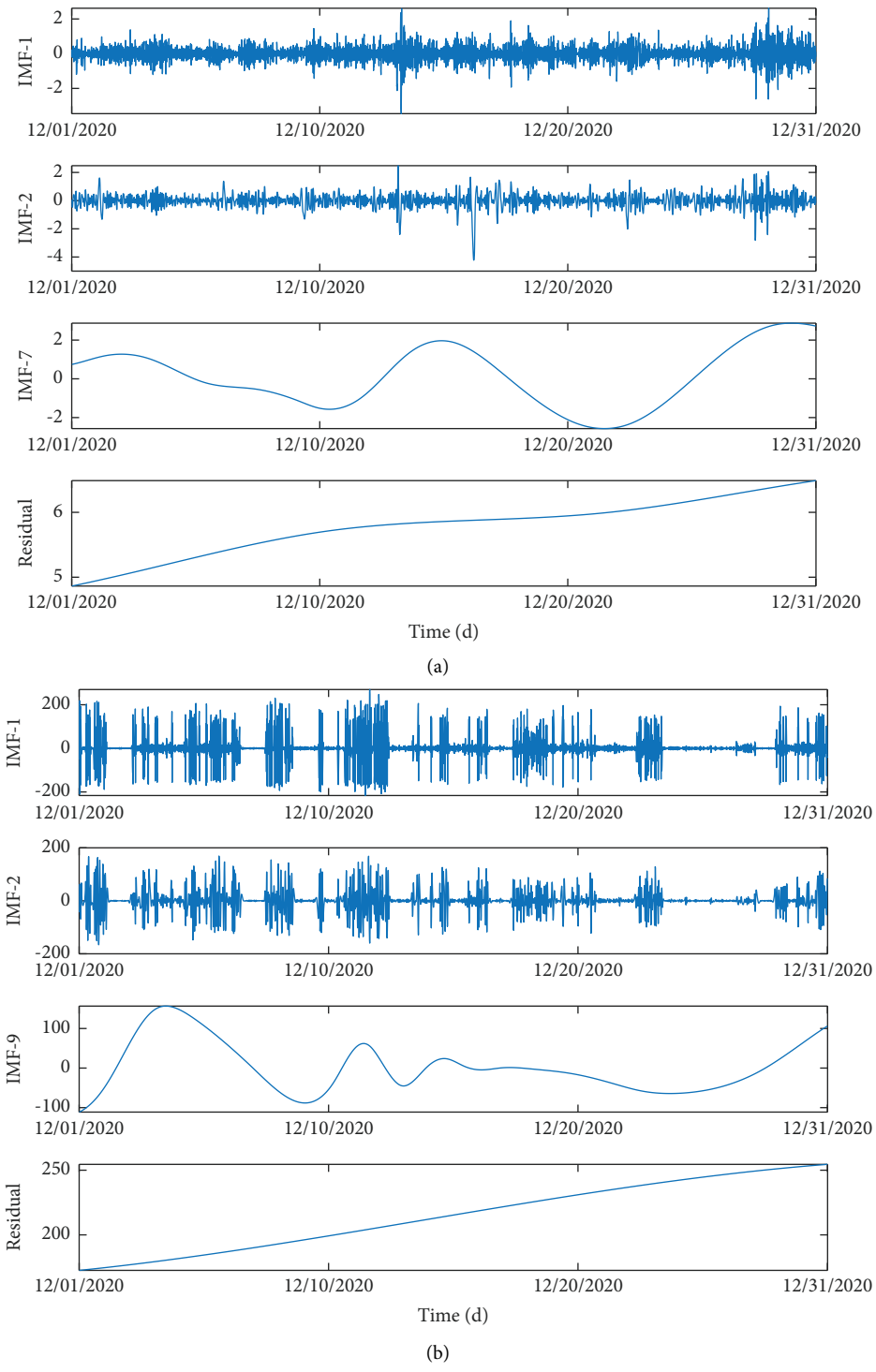


Figure 5: EMD of the wind monitoring data. (a) Wind speed decomposition. (b) Wind direction decomposition.

the wind speed exceeded 17 m/s. The collected wind speed can effectively represent the wind speed changes in daily operations. In addition, the wind direction data show obvious uncertainty, i.e., it has large fluctuations. In particular, the wind direction of the Jiashao Bridge in the study month is mainly northwest, which is mainly related to winter weather.

In addition, to better discuss the wind dataset, we have performed statistical analysis of the wind speed and direction, respectively (Ding et al. [38]). As shown in Figure 4(a), the statistical probability distribution of wind speed has two peaks, 5 and 12 m/s. Specifically, the 5 m/s peak refers to the daily wind speed, and the 12 m/s peak refers to the impact of gale weather. That is, the Jiashao

Bridge was less affected by the strong wind in December 2020, and the collected wind speed data can represent the daily wind speed changes. Therefore, the change in wind speed has some regularity and can be accurately predicted. In contrast, the wind direction is mainly concentrated between 300° and 360°, as shown in Figure 4(b). Furthermore, the statistical probability distribution of the wind direction has multipeak characteristics, i.e., strong random characteristics, which will lead to difficulties in wind direction prediction.

*3.2. Data Preprocessing.* First, the wind monitoring data are denoised, i.e., the EMD method is used to decompose and reconstruct the wind speed and direction, as shown in Figure 5. As shown in Figure 5(a), the wind speed is decomposed into seven IMFs and one residual. Specifically, the IMF-1 displays the high-order frequency of wind speed, and the residual represents the trend term of wind speed. As shown in Figure 5(b), the wind direction is decomposed into nine IMFs and one residual. Specifically, the IMF-1 displays the high-order frequency of wind direction, which is more random and uncertain compared to wind speed. Similarly, the residual represents the trend term of the wind direction.

Specifically, the relative tolerance between IMF components and the wind speed is shown in Table 1. The relative tolerance between the IMF components and the wind direction is shown in Table 2. Specially, the relative tolerance is a Cauchy-type stop criterion in the EMD method, the sifting stops when current relative tolerance is less than relative tolerance.

Furthermore, we conduct Pearson correlation tests on the obtained IMF, residual, and raw data (wind speed and direction), as shown in Tables 3 and 4. As can be seen in Table 3, the IMF-6 and IMF-7 have the best correlation with wind speed, and these two components can be used to represent the trend of wind speed changes. Similarly, the IMF-6 has the best correlation with the wind direction, and this component can be used to represent the trend of wind direction changes as shown in the Table 4.

Finally, the wind speed and direction data were reconstructed, as shown in Figure 6. Figure 6 shows that the reconstructed wind speed and direction data can maintain the characteristics of the original wind data. The data also exclude some abnormal data, such as noise data. Therefore, we can obtain high-quality monitoring data using the EMD method.

*3.3. Case Study 1: Prediction of the Direct Method.* In this paper, the dataset is divided into three categories in LSTM model: training set is 80% of the dataset, validation set is 10% of the dataset, and test set is 10% of the dataset at first. Then, the Adam optimizer is used to train model to obtain the best parameter (weight and offset), the learning rate is 0.001, and the error function is mean squared in the LSTM model. In which, the conditions for stopping training or predicting of LSTM model are: (1) the model meet the set accuracy requirements, that is, the minimum error is set to $10^{-6}$. (2) The model reached the maximum number of iterations, that is, the number of iterations is set to 100. In addition, the dataset is full used based on cross-validation method, which can avoid the model from under fitting or over fitting (Bokde et al. [39]).

Table 1: Relative tolerance between IMF components and wind speed.

| IMF | Relative tolerance |
|---|---|
| IMF-1 | 0.138 |
| IMF-2 | 0.031 |
| IMF-3 | 0.092 |
| IMF-4 | 0.088 |
| IMF-5 | 0.056 |
| IMF-6 | 0.016 |
| IMF-7 | 0.003 |

Table 2: Relative tolerance between IMF components and wind direction.

| IMF | Relative tolerance |
|---|---|
| IMF-1 | 0.054 |
| IMF-2 | 0.053 |
| IMF-3 | 0.099 |
| IMF-4 | 0.037 |
| IMF-5 | 0.055 |
| IMF-6 | 0.117 |
| IMF-7 | 0.090 |
| IMF-8 | 0.034 |
| IMF-9 | 0.069 |

Table 3: Correlation coefficient between IMF components and wind speed.

| IMF | Correlation coefficient |
|---|---|
| IMF-1 | 0.138 |
| IMF-2 | 0.151 |
| IMF-3 | 0.244 |
| IMF-4 | 0.264 |
| IMF-5 | 0.332 |
| IMF-6 | 0.610 |
| IMF-7 | 0.531 |
| Residual | 0.145 |

Table 4: Correlation coefficient between IMF components and wind direction.

| IMF | Correlation coefficient |
|---|---|
| IMF-1 | 0.415 |
| IMF-2 | 0.240 |
| IMF-3 | 0.177 |
| IMF-4 | 0.009 |
| IMF-5 | 0.317 |
| IMF-6 | 0.497 |
| IMF-7 | 0.375 |
| IMF-8 | 0.429 |
| IMF-9 | 0.081 |
| Residual | −0.043 |

The closer the correlation coefficient is to 1, the stronger correlation between the IMF component and the original data.

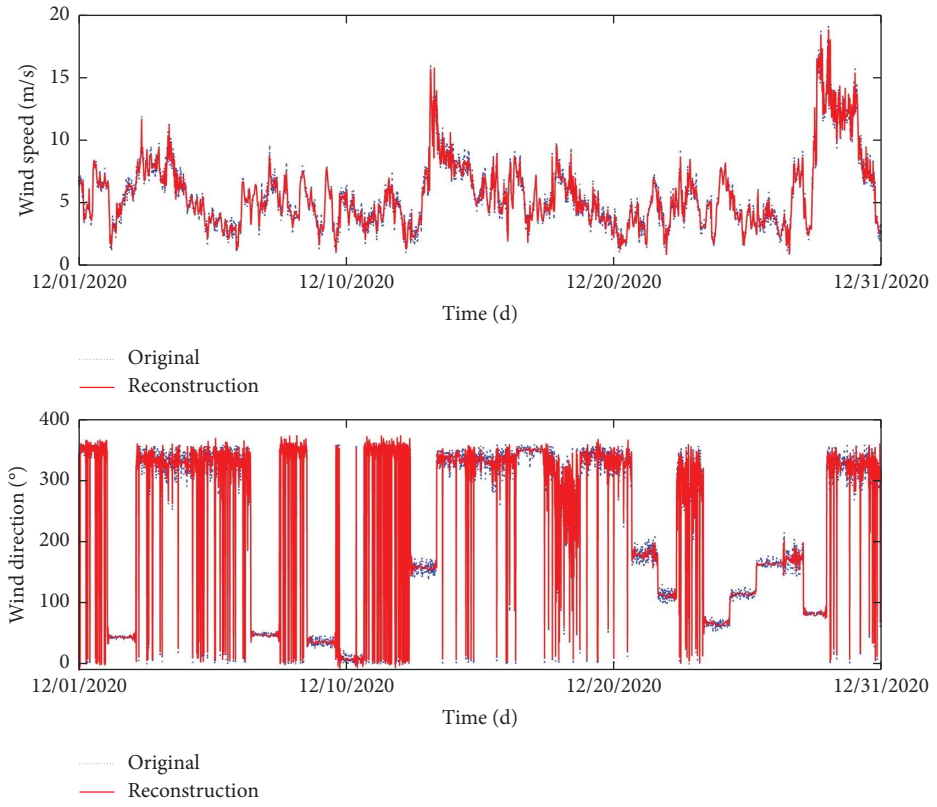


Figure 6: Reconstruction and the original wind data.

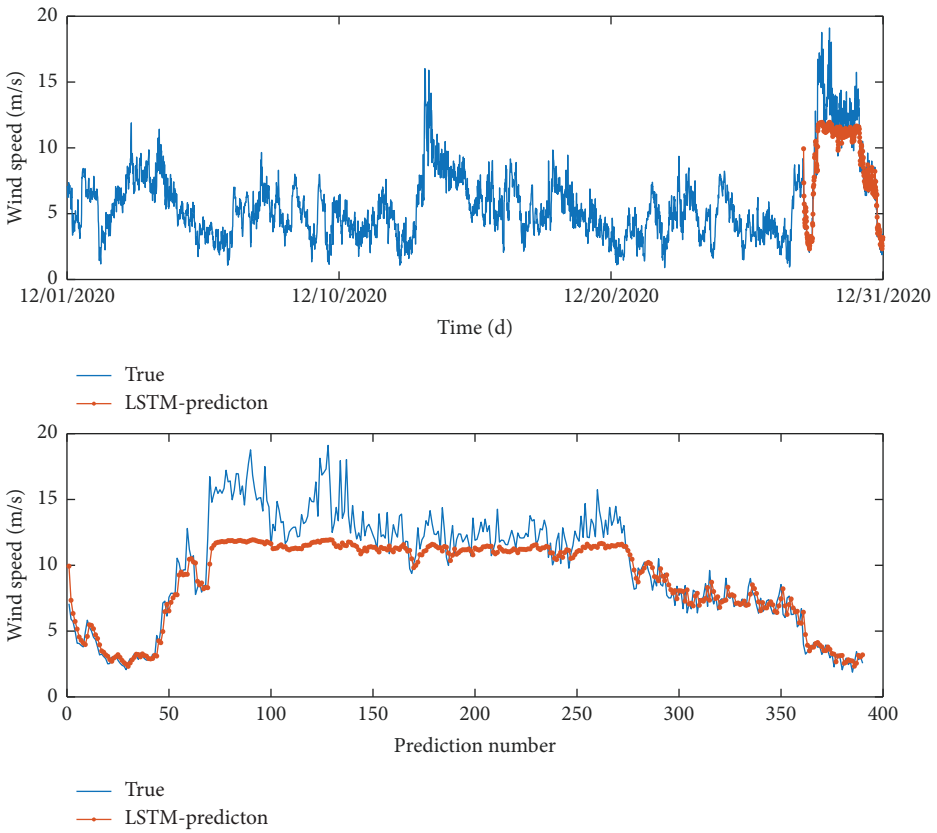


Figure 7: Wind speed prediction based on direct method.

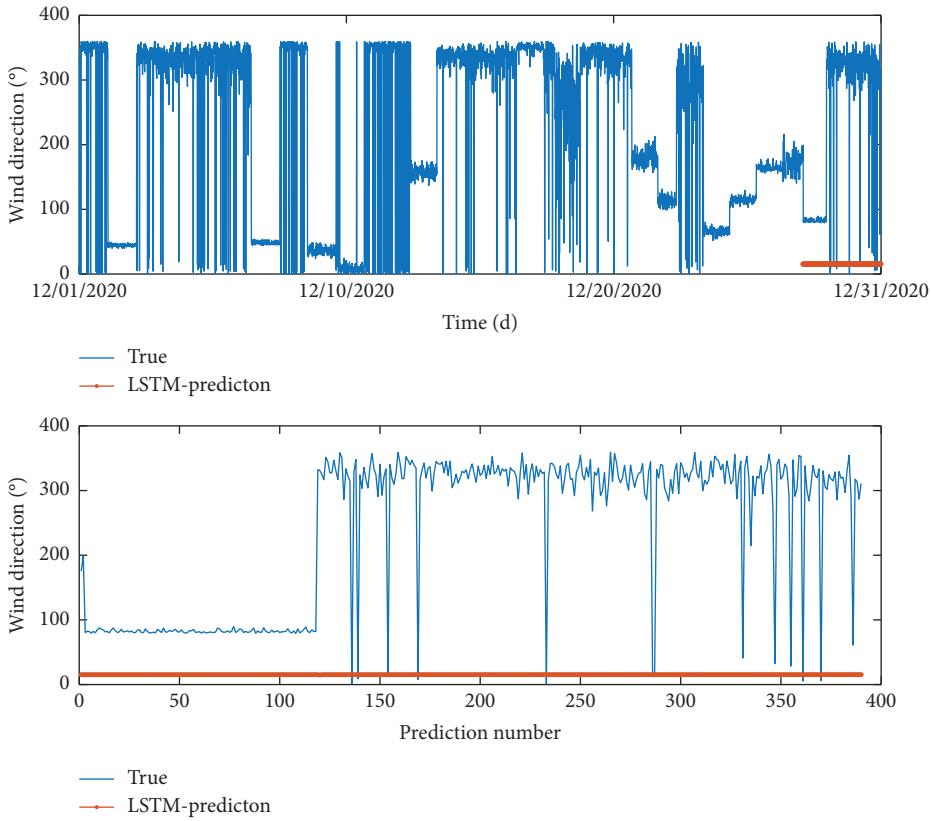


Figure 8: Wind direction prediction based on direct method.

In particular, we use a direct method to predict the wind speed and direction in case study 1, i.e., the LSTM model is used to directly predict the wind speed and direction in a multistep approach. For the LSTM model, the number of hidden layer nodes is 32, and the number of steps is 10. As shown in subfigure-1 of Figure 7, the direct method can predict the trend of changes in wind speed. Furthermore, the prediction performance of wind speed is very good; that is, its RMSE value is 0.6148, as shown in subfigure-2 of Figure 7. However, the direct method cannot predict the change law and the specific value of wind direction; that is, the direct method cannot be applied to the wind direction prediction, as shown in Figure 8.

*3.4. Case Study 2: Prediction of the Indirect Method.* In the case study 2, we try to use LSTM model to predict the wind direction based on indirect method. First, we can see that the LSTM model has a good prediction effect on wind speed in the case study 1. Therefore, we decompose the wind speed into the crosswind speed and alongwind speed with considering the correlation between the wind speed and wind direction, as shown in Figure 9.

Specifically, the relationship between crosswind speed, alongwind speed, and wind direction can be expressed as follows:

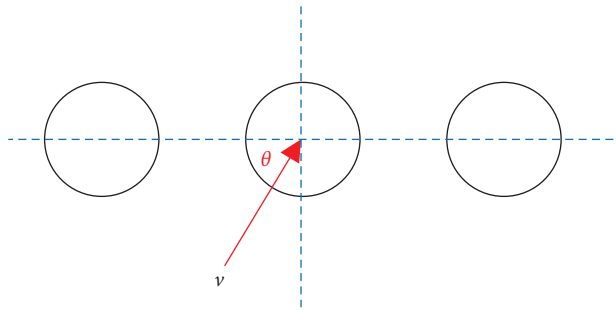


Figure 9: Wind effect considering the wind direction.

$$\begin{aligned} v_{\text{cross}} &= v \times \sin(\theta), \\ v_{\text{along}} &= v \times \cos(\theta), \\ \theta &= \arctan\left(\frac{v_{\text{cross}}}{v_{\text{along}}}\right), \\ v &= \sqrt{v_{\text{cross}}^2 + v_{\text{along}}^2}, \end{aligned} \tag{4}$$

where $v$ represents the total wind speed; $v_{\text{cross}}$ denotes the crosswind speed; $v_{\text{along}}$ denotes the alongwind speed; and $\theta$ denotes the wind direction.

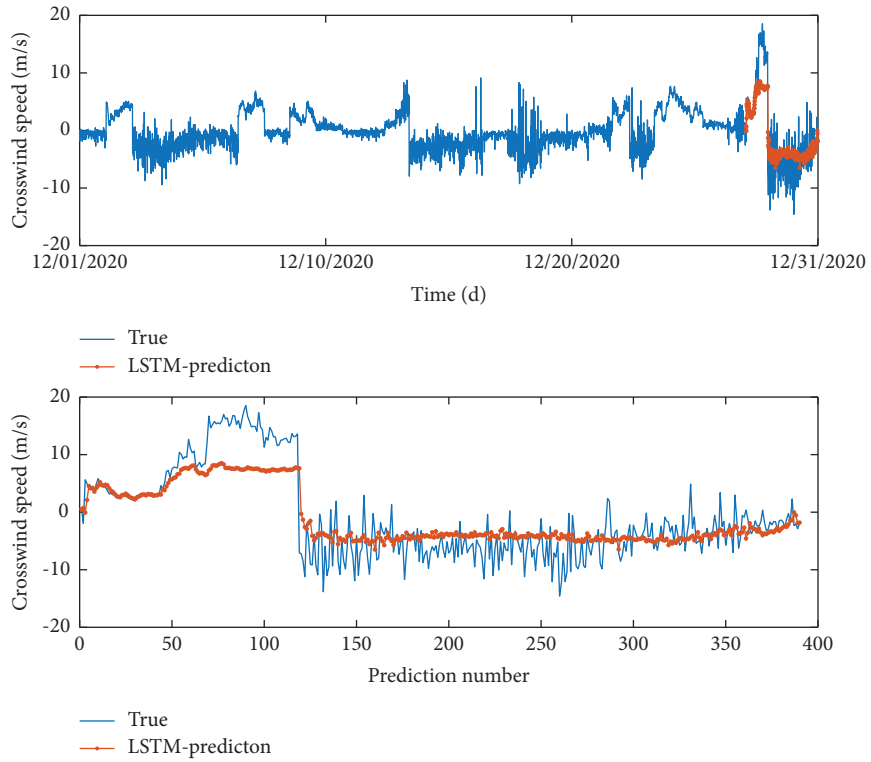


Figure 10: Crosswind speed prediction.

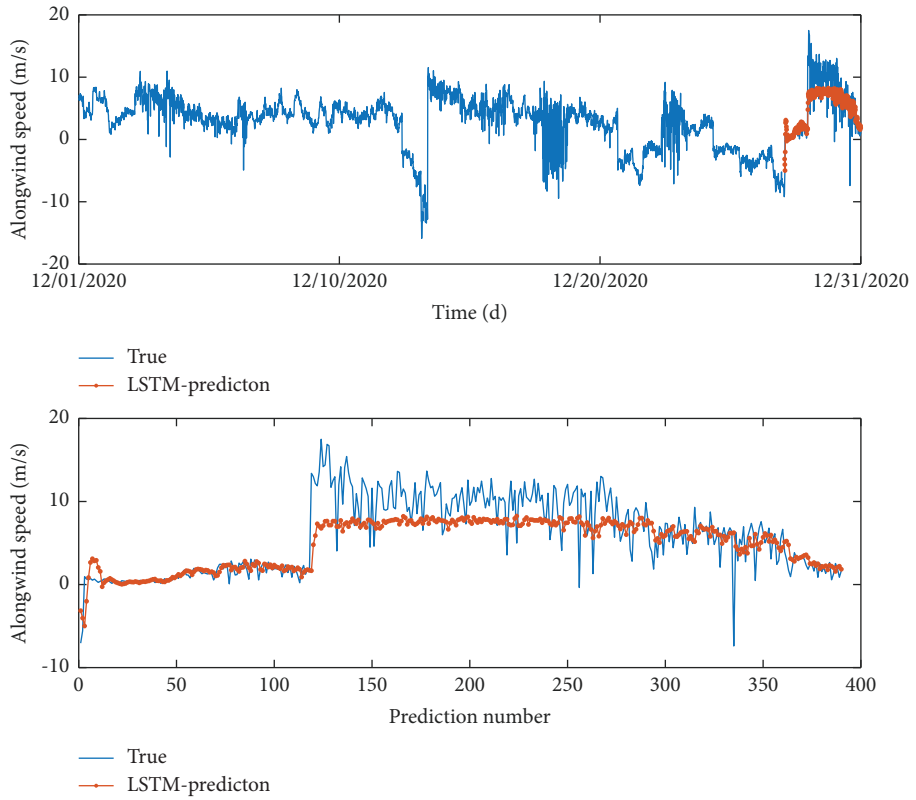


Figure 11: Alongwind speed prediction.

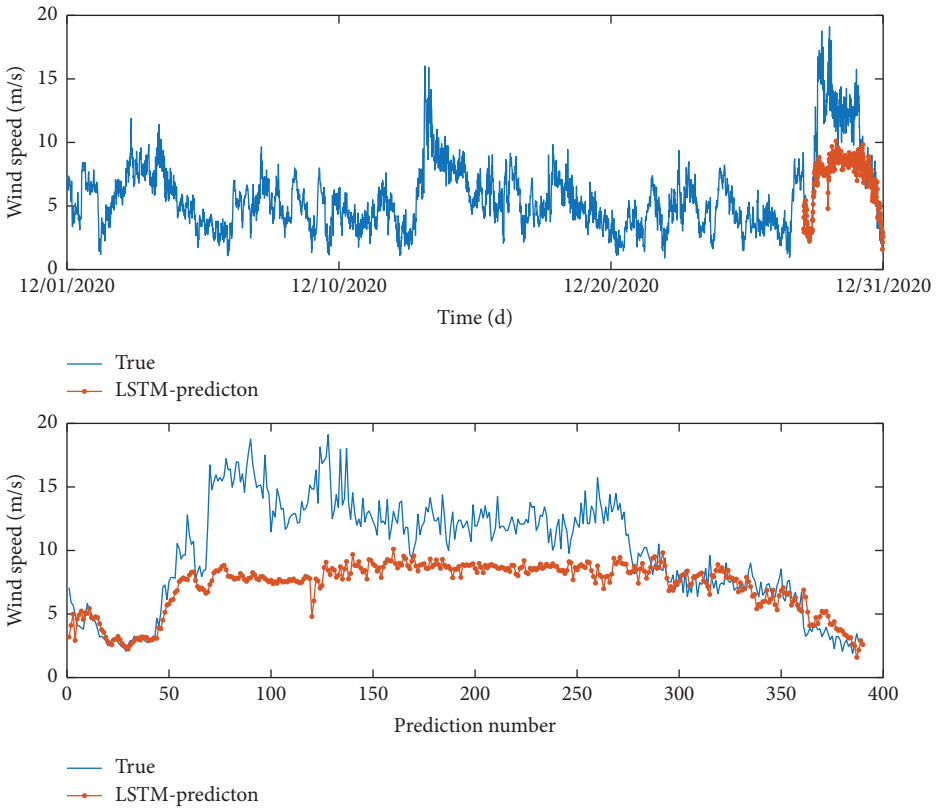


Figure 12: Wind speed prediction based on indirect method.

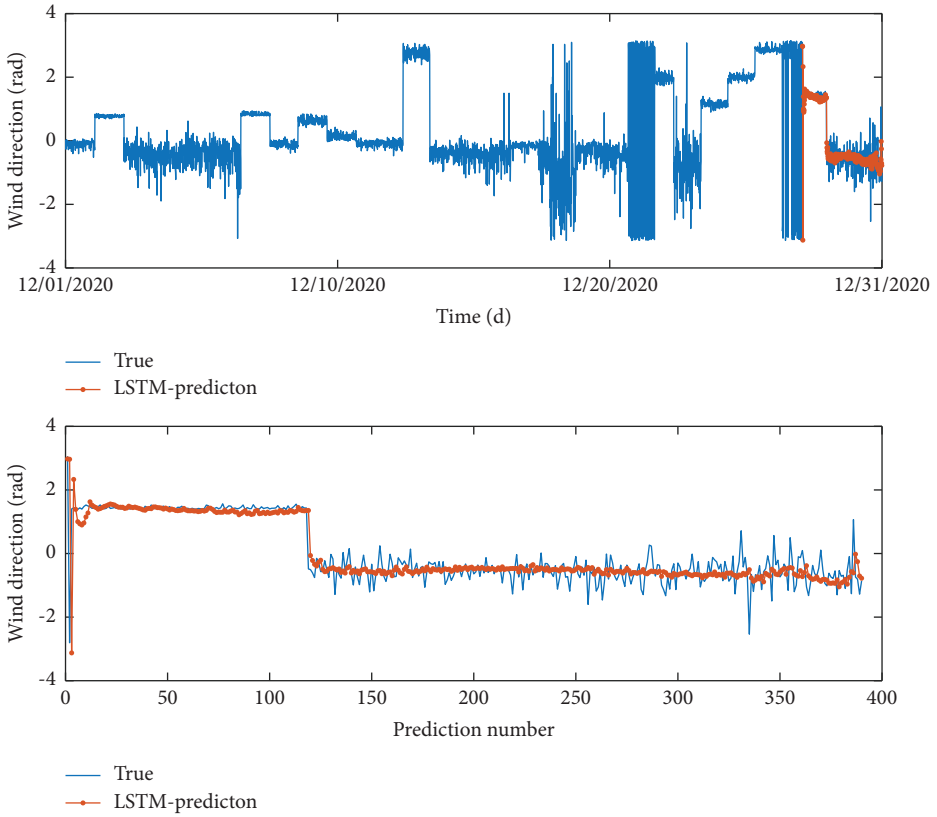


(a)

Figure 13: Continued.

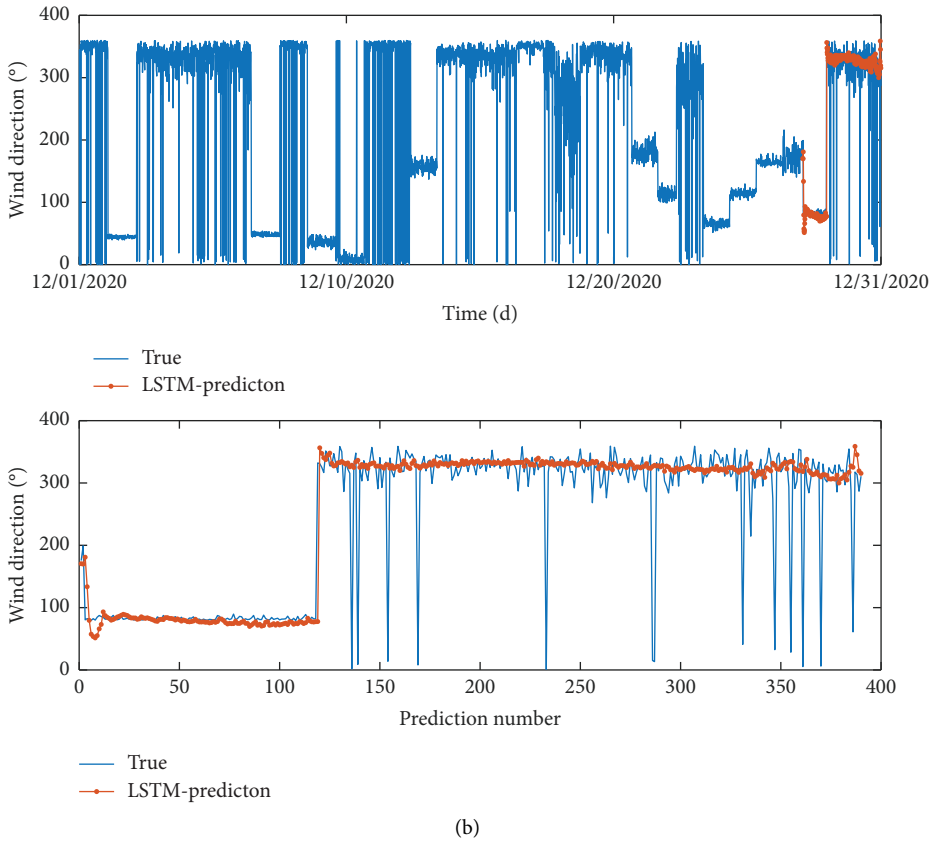


(b)

Figure 13: Wind direction prediction based on indirect method. (a) Wind direction-radian prediction. (b) Wind direction-angle prediction.

Furthermore, the crosswind speed and alongwind speed are predicted based on LSTM model, respectively, as shown in Figures 10 and 11. In addition, the parameter settings and training process in the LSTM model are the same as in case study 1. Specially, the indirect method can predict the change trend of crosswind speed and alongwind speed as can be seen from subfigure-1 of Figures 10 and 11. The LSTM model has good prediction performance for the crosswind speed and alongwind speed, and their RMSE values are 1.2524 and 0.9151, respectively, as can be seen from subfigure-2 of Figures 10 and 11.

Based on the equation (4), the total wind speed prediction can be calculated, as shown in Figure 12. It can be seen from the subfigure-1 of Figure 12, although the indirect method can predict the change trend and value of wind speed. But its prediction performance is very poor as can be seen from subfigure-2 of Figure 12, that is, its RMSE value is 3.9489. This is because the crosswind speed and alongwind speed have errors in the prediction process, and then the prediction error of total wind speed is greater due to the accumulation of errors. Therefore, it is suggested to use the direct method to predict wind speed.

In addition, the wind direction prediction can be calculated based on the equation (4), as shown in Figure 13(a). In particular, we used the radian (rad) wind direction data to express the angle wind direction data because of the tangent function is periodic, and the *a*tan2 function in MATLAB requires the value (wind direction) between $-\pi$ and $\pi$. As can be seen from Figure 13(b), the indirect method can predict the change trend of wind direction in the subfigure-1, and the prediction performance of wind speed is good in the subfigure-2, that is, its RMSE value is 0.520.

## 4. Conclusions

In this study, a wind speed and direction prediction model is proposed on the basis of direct and indirect methods. Specifically, the wind speed is decomposed into crosswind and alongwind speeds considering the correlation between the wind speed and direction. In addition, the wind speed and direction data were denoised by EMD. The crosswind and alongwind speeds are predicted using an LSTM model, and then, the wind direction is predicted. Based on the SHM data, collected from the study bridge, the effectiveness of direct and indirect predictions of wind speed and direction is verified. Some conclusions are as follows: (1) the LSTM model based on a direct or an indirect method can predict the change trend and value of wind speed, which is verified using SHM data. The LSTM wind speed prediction model based on the direct method outperforms that based on the indirect method. Therefore, it is suggested to use a direct method for wind speed prediction. (2) The LSTM model based on the direct method is unsuitable for wind direction prediction; that is, it cannot predict the change trend and value of wind direction. The LSTM model based on an indirect method can predict the change trend and

value of wind direction and has good prediction performance, which is verified using SHM data. Therefore, it is suggested to use an indirect method for wind direction prediction.

## Appendix

## A. Meaning of Variables

This appendix lists the variables in the equations, which include twenty-one variables symbol, that is,

$P(t)$ denotes the SHM data

$y_i(t)$ denotes the $i$th IMF

$l_n(t)$ denotes the Residual value

$i$ denotes the input gate

$W_i$ denotes the weight of the input gate

$b_i$ denotes the offset of the input gate

$f$ denotes the forgetting gate

$W_f$ denotes the weight of the forgetting gate

$b_f$ denotes the offset of the forgetting gate

$o$ denotes the output gate

$W_o$ denotes the weight of the output gate

$b_o$ denotes the offset of the output gate

$x_t$ denotes the unit input

$z_t$ denotes the status of a temporary unit

$W_z$ denotes the weight of the status of the temporary unit

$b_z$ denotes the offset of the status of the temporary unit

$c_t$ denotes the current unit state

$c_{t-1}$ denotes the status of the previous unit

$h_t$ denotes the hidden state of the current unit

$h_{t-1}$ denotes the hidden state of the previous unit

$N$ denotes the size of the test set sample

## B. Phrase Abbreviations

This appendix lists the abbreviations in this paper, which include seven abbreviations, that is,

Long short-term memory: LSTM

Empirical mode decomposition: EMD

Structural health monitoring: SHM

Artificial neural network: ANN

Intrinsic mode functions: IMF

Root mean square error: RMSE

Ultrasonic anemometer: UAN

## Data Availability

Some or all the data, models, or code that support the findings of this study are available from the corresponding author upon reasonable request.

## Conflicts of Interest

The authors declare that they have no conflicts of interest.

## Authors' Contributions

Y. Ding performed the methodology and wrote, reviewed, and edited the original draft. X. W. Ye conceptualized and supervised the study. Y. Guo performed the supervision.

## Acknowledgments

The work described in this paper was jointly supported by the Scientific Research Project of the Zhejiang Provincial Department of Education (grant no. Y202248682), Educational Science Planning Project of Zhejiang Province (grant no. 2023SCG222), National Natural Science Foundation of China (grant no. 52178306), and Zhejiang Provincial Natural Science Foundation (grant no. LR19E080002).

## References

[1] X. W. Ye, Y. Ding, and H. P. Wan, "Machine learning approaches for wind speed forecasting using long-term monitoring data: a comparative study," *Smart Structures and Systems*, vol. 24, no. 6, pp. 733–744, 2019a.

[2] X. W. Ye, Y. Ding, and H. P. Wan, "Probabilistic forecast of wind speed based on bayesian emulator using monitoring data," *Structural Control and Health Monitoring*, vol. 28, no. 1, Article ID e2650, 2021.

[3] W. M. Zhang, Z. W. Wang, and Z. Liu, "Joint distribution of wind speed, wind direction, and air temperature actions on long-span bridges derived via trivariate metaelliptical and Plackett copulas," *Journal of Bridge Engineering*, vol. 25, no. 9, Article ID 04020069, 2020.

[4] S. Li, S. Li, S. Laima, and H. Li, "Data-driven modeling of bridge buffeting in the time domain using long short-term memory network based on structural health monitoring," *Structural Control and Health Monitoring*, vol. 28, no. 8, Article ID e2772, 2021.

[5] W. Xu, P. Liu, L. Cheng et al., "Multi-step wind speed prediction by combining a WRF simulation and an error correction strategy," *Renewable Energy*, vol. 163, pp. 772–782, 2021a.

[6] Z. Ye, N. Li, and F. Zhang, "Wind characteristics and responses of Xihoumen Bridge during typhoons based on field monitoring," *Journal of Civil Structural Health Monitoring*, vol. 9, no. 1, pp. 1–20, 2019.

[7] Y. Zhou and L. Sun, "Effects of high winds on a long-span sea-crossing bridge based on structural health monitoring," *Journal of Wind Engineering and Industrial Aerodynamics*, vol. 174, pp. 260–268, 2018.

[8] H. Li, J. Ou, X. Zhao et al., "Structural health monitoring system for the Shandong Binzhou Yellow River highway bridge," *Computer-Aided Civil and Infrastructure Engineering*, vol. 21, no. 4, pp. 306–317, 2006.

[9] Y. Shao, C. Miao, B. Li, and Q. Wu, "Simultaneous de-noising and enhancement method for long-span bridge health monitoring data based on empirical mode decomposition and fractal conservation law," *Measurement Science and Technology*, vol. 30, no. 6, Article ID 065103, 2019.

[10] J. Hu, J. Wang, and G. Zeng, "A hybrid forecasting approach applied to wind speed time series," *Renewable Energy*, vol. 60, pp. 185–194, 2013.

[11] C. Wu, J. Wang, X. Chen, P. Du, and W. Yang, "A novel hybrid system based on multi-objective optimization for wind speed forecasting," *Renewable Energy*, vol. 146, pp. 149–165, 2020.

[12] H. Hu, J. Zhang, and T. Li, "A comparative study of VMD-based hybrid forecasting model for nonstationary daily streamflow time series," *Complexity*, vol. 2020, p. 21, 2020.

[13] P. Pandey, N. D. Bokde, S. Dongre, and R. Gupta, "Hybrid models for water demand forecasting," *Journal of Water Resources Planning and Management*, vol. 147, no. 2, Article ID 04020106, 2021.

[14] Z. Qian, Y. Pei, H. Zareipour, and N. Chen, "A review and discussion of decomposition-based hybrid models for wind energy forecasting applications," *Applied Energy*, vol. 235, pp. 939–953, 2019.

[15] N. Bokde, A. Feijóo, D. Villanueva, and K. Kulat, "A review on hybrid empirical mode decomposition models for wind speed and wind power prediction," *Energies*, vol. 12, no. 2, 2019.

[16] X. Liu, Z. Lin, and Z. Feng, "Short-term offshore wind speed forecast by seasonal ARIMA-A comparison against GRU and LSTM," *Energy*, vol. 227, Article ID 120492, 2021.

[17] F. Shahid, A. Zameer, A. Mehmood, and M. A. Z. Raja, "A novel wavenets long short term memory paradigm for wind power prediction," *Applied Energy*, vol. 269, Article ID 115098, 2020.

[18] H. Liu, X. Mi, Y. Li, Z. Duan, and Y. Xu, "Smart wind speed deep learning based multi-step forecasting model using singular spectrum analysis, convolutional gated recurrent unit network and support vector regression," *Renewable Energy*, vol. 143, pp. 842–854, 2019.

[19] H. Liu, H. Q. Tian, D. F. Pan, and Y. F. Li, "Forecasting models for wind speed using wavelet, wavelet packet, time series and Artificial Neural Networks," *Applied Energy*, vol. 107, pp. 191–208, 2013.

[20] S. Jung and S. D. Kwon, "Weighted error functions in artificial neural networks for improved wind energy potential estimation," *Applied Energy*, vol. 111, pp. 778–790, 2013.

[21] Z. Guo, J. Zhao, W. Zhang, and J. Wang, "A corrected hybrid approach for wind speed prediction in Hexi Corridor of China," *Energy*, vol. 36, no. 3, pp. 1668–1679, 2011.

[22] X. W. Ye, P. S. Xi, Y. H. Su, B. Chen, and J. P. Han, "Stochastic characterization of wind field characteristics of an arch bridge instrumented with structural health monitoring system," *Structural Safety*, vol. 71, pp. 47–56, 2018.

[23] B. P. Alduse, S. Jung, O. A. Vanli, and S. D. Kwon, "Effect of uncertainties in wind speed and direction on the fatigue damage of long-span bridges," *Engineering Structures*, vol. 100, pp. 468–478, 2015.

[24] Y. Ding, S. X. Zhou, Y. Q. Wei, T. L. Yang, and J. L. Dong, "Influence of wind speed, wind direction and turbulence model for bridge hanger: a case study," *Symmetry*, vol. 13, no. 9, 2021.

[25] J. X. Wang, C. M. Ma, M. Li, N. Yeung, and S. Li, "Experimental and numerical studies of the vortex-induced vibration behavior of an asymmetrical composite beam bridge," *Advances in Structural Engineering*, vol. 22, no. 10, pp. 2236–2249, 2019.

[26] H. Xiang, Y. Li, S. Chen, and G. Hou, "Wind loads of moving vehicle on bridge with solid wind barrier," *Engineering Structures*, vol. 156, pp. 188–196, 2018.

[27] H. N. Li, X. W. Zheng, and C. Li, "Copula-based joint distribution analysis of wind speed and direction," *Journal of Engineering Mechanics*, vol. 145, no. 5, Article ID 04019024, 2019.

[28] H. Wang, T. Y. Tao, T. Wu, J. Mao, and A. Li, "Joint distribution of wind speed and direction in the context of field measurement," *Wind and Structures*, vol. 20, no. 5, pp. 701–718, 2015.

[29] X. Zhang and X. Chen, "Assessing probabilistic wind load effects via a multivariate extreme wind speed model: a unified framework to consider directionality and uncertainty," *Journal of Wind Engineering and Industrial Aerodynamics*, vol. 147, pp. 30–42, 2015.

[30] Z. Qu, W. Mao, K. Zhang, W. Zhang, and Z. Li, "Multi-step wind speed forecasting based on a hybrid decomposition technique and an improved back-propagation neural network," *Renewable Energy*, vol. 133, pp. 919–929, 2019.

[31] Y. Amirat, V. Choqueuse, and M. Benbouzid, "Eemd-based wind turbine bearing failure detection using the generator stator current homopolar component," *Mechanical Systems and Signal Processing*, vol. 41, no. 1-2, pp. 667–678, 2013.

[32] X. Meng, H. Fu, L. Peng et al., "D-LSTM: short-term road traffic speed prediction model based on GPS positioning data," *IEEE Transactions on Intelligent Transportation Systems*, vol. 23, no. 3, pp. 2021–2030, 2022.

[33] Z. Yuan, J. Liu, Q. Zhang, Y. Liu, Y. Yuan, and Z. Li, "Prediction and optimisation of fuel consumption for inland ships considering real-time status and environmental factors," *Ocean Engineering*, vol. 221, Article ID 108530, 2021.

[34] X. Xu, Y. L. Xu, Y. Ren, and Q. Huang, "Site-specific extreme load estimation of a long-span cable-stayed bridge," *Journal of Bridge Engineering*, vol. 26, no. 4, Article ID 05021001, 2021.

[35] Z. Zhang, L. Ye, H. Qin et al., "Wind speed prediction method using shared weight long short-term memory network and Gaussian process regression," *Applied Energy*, vol. 247, pp. 270–284, 2019.

[36] X. W. Ye, Y. Ding, and H. P. Wan, "Statistical evaluation of wind properties based on long-term monitoring data," *Journal of Civil Structural Health Monitoring*, vol. 10, no. 5, pp. 987–1000, 2020.

[37] Y. Ding, X. W. Ye, and Y. Guo, "Data set from wind, temperature, humidity and cable acceleration monitoring of the Jiashao bridge," *Journal of Civil Structural Health Monitoring*, vol. 13, no. 2-3, pp. 579–589, 2023.

[38] Y. Ding, X. W. Ye, and Y. Guo, "Wind load assessment with the JPDF of wind speed and direction based on SHM data," *Structures*, vol. 47, no. 1, pp. 2074–2080, 2023.

[39] N. D. Bokde, Z. M. Yaseen, and G. B. Andersen, "ForecastTB-An R package as a test-bench for time series forecasting-application of wind speed and solar radiation modeling," *Energies*, vol. 13, no. 10, 2020.